JOURNAL OF SPACECRAFT AND ROCKETS
Vol. 46, No. 2, March–April 2009

Practical Systems Design for an Earth-Magnetotail-Monitoring Solar Sail Mission

Vaios Lappas*
University of Surrey, Guildford, England GU2 7XH, United Kingdom
Giovanni Mengali† and Alessandro A. Quarta‡
University of Pisa, 56122 Pisa, Italy
Jesus Gil-Fernandez§
GMV, GmbH, 28760 Madrid, Spain
Tilo Schmidt¶
HTS, GmbH, 01640 Saxony, Germany
and
Bong Wie**
Iowa State University, Ames, Iowa 50011

DOI: 10.2514/1.32040

Solar sails are currently being studied and developed as alternate propulsion vehicles that can provide high velocities. Their ability to reflect photons coming from the sun on a large lightweight reflective surface enables many unique space science missions. One such mission is the GeoSail mission, for which the aim is the study of Earth's magnetotail. Recent advances in solar sail technologies, satellite bus miniaturization, and attitude control motivate the present study of an alternate systems design approach for GeoSail. This paper details a practical systems approach toward the design of a 40 × 40 m sail, focusing on the design and use of niche enabling technologies with applications to the proposed GeoSail mission. The study is based on mission and system design requirements from ESA's technology reference studies, which focus on the development of strategically important technologies in preparation of future scientific missions: in this case, for the 2015–2025 time frame.

Nomenclature

A	=	sail area, m^2
a	=	semimajor axis, km
$\mathbf{a}$	=	sail characteristic acceleration vector, mm/s^2
a_c	=	sail characteristic acceleration, mm/s^2
$a_{c_{des}}$	=	dimensionless sail characteristic acceleration
a_r	=	radial component of the sail acceleration, mm/s^2
a_t	=	transverse component of the sail acceleration, mm/s^2
b_1, b_2, b_3	=	sail optical coefficients
E	=	Young's modulus, N/mm^2
e	=	eccentricity
F_b	=	boom tip bending force, N
F_t	=	total force, N
f	=	boom deflection, mm
f_s	=	shadow function
I	=	moment of inertia of the cross section, $kg \cdot m^2$
I_{TI}	=	total torque impulse, $N \cdot m \cdot s$
I_i	=	total impulse, s
J	=	performance index
L	=	length of the cross section, mm
l_b	=	boom length, m
$m_{CFRP_{length}}$	=	mass per length, g/m
$m_{CFRP_{spec}}$	=	specific mass, g/m^2
m_f	=	film mass, g
m_{matrix}	=	matrix mass, g
m_{struc}	=	boom structure mass, g
M_{tip}	=	tip thruster mass, g
$N_{control}$	=	control torque, $N \cdot m$
$N_{SRP\text{-}D}$	=	solar-radiation-pressure disturbance torque, $N \cdot m$
R	=	allowable bending force, N
r	=	Earth-sail distance, km
s	=	traveling distance, km
$\dot{\delta}$	=	sun-line rotation, deg /day
η	=	control parameter
η_s	=	sail efficiency
θ	=	attitude error angle, deg
μ	=	Earth's gravitational constant, km^3/s^2
ν	=	true anomaly, deg
ρ	=	blanket substrate density, kg/m^3
σ	=	sail loading, g/m^2
ω	=	argument of perigee, deg
$\dot{\omega}$	=	apse-line rotation rate, deg /day

Received 8 May 2007; revision received 12 January 2009; accepted for publication 12 January 2009.

*Senior Lecturer; V.Lappas@surrey.ac.uk. Member AIAA.
†Associate Professor, Department of Aerospace Engineering; g.mengali@ing.unipi.it. Member AIAA.
‡Research Fellow, Department of Aerospace Engineering; a.quarta@ing.unipi.it. Senior Member AIAA.
§Mission Analyst; jesusgil@gmv.es.
¶Structural Engineer; tilo.schmidt@htsdd.de.
**Vance Coffman Professor; bongwie@iastate.edu. Associate Fellow AIAA.

I. Introduction

FOR more than two decades, scientists and engineers considered the use of sails for space exploration. The terrestrial counterpart, wind sails, carried human exploration on Earth to the far edges of humanity and discovery. Similarly, many scientists in the space community have studied the idea of using solar pressure as the wind to propel a spacecraft, similar to a sailboat, to the far edges of our solar system and beyond. The GeoSail mission for the Earth's magnetotail study is a mission concept previously researched by NASA and ESA. Recent advances in solar sail technologies, satellite bus miniaturization, and attitude control motivate the present study of an alternate GeoSail design. Technology reference studies (TRS)

introduced by ESA focus on the development of strategically important technologies in preparation of future scientific missions. A number of TRS have been successfully studied in the context of ESA's scientific Cosmic Vision 2015–2025 [1]. Although the work presented in this paper is not directly associated with ESA's original work, it does employ the TRS parameters to establish realistic mission design requirements [1,2]. Previous studies and proposals considered the spin-stabilized heliogyro configuration for the visit of comet Halley in 1986 and interplanetary solar sail missions in our solar system and the heliopause. The Science Payload and Advanced Concept Office identified GeoSail as a potential future ESA scientific mission. GeoSail employs a 40×40 m solar sail that can be used to artificially precess the apse line of its 11×23 Earth-radii reference orbit. As a result, a miniature science payload is stationed within the geomagnetic tail, providing periodic science returns. The long-term residence of the payload in the geomagnetic tail allows phenomena, such as magnetic reconnection, to be studied in situ. Using multiple solar sails, the entire geomagnetic tail could be populated by sensors that precess with the annual rotation of the geomagnetic tail, allowing real-time visualization of the 3-D plasma structure of the geomagnetic tail [1,3–5].

This paper details a practical system approach toward the design of a 40×40 m sail, focusing on the design and use of niche enabling technologies for the proposed GeoSail mission. The niche and differentiating technologies analyzed compared with previous work are [1–7] as follows:

1) Mission analysis and tradeoff of propulsion technologies are needed to place the solar sail spacecraft in the GeoSail orbit.

2) A novel and more realistic sail steering law is used for solar sail design, which includes solar sail degradation as well as eclipse and shadowing effects.

3) An innovative solar sail design is based on the in-orbit bonding (IOB) technology, along with its benefits in boom rigidity and sail mass savings.

4) A practical and robust attitude control system is compact and provides increased redundancy.

5) The use of ultraminiature and low-cost small-satellite design technologies reduces the total mission mass and cost based on significant heritage of small-satellite missions.

II. Mission Analysis

GeoSail is a low-cost innovative mission for which the main purpose is to demonstrate solar sails as a feasible propulsion concept [3–5]. It was devised by Macdonald and McInnes [3] in 2000 and then refined in other papers [2,4–7]. Within this mission, a solar sail is used to precess the apse line of an elliptical orbit for which the major axis lies along the Earth's geomagnetic tail. The precession rate is chosen such that the orbit apogee remains continuously in the geomagnetic tail, thus allowing for long-duration magnetospheric plasma research [3–5]. In the work presented here, the proposed operational scenario considers the solar sail spacecraft transported to its main elliptical orbit with a transfer vehicle. The design of the transfer trajectory and the characteristics of the associated vehicle are presented in Sec. III. The sail is assumed to be deployed after separation from the transfer vehicle. In addition, the sail deployment mechanism is subsequently ejected to minimize mass.

Beyond GeoSail, other solar sail concepts for space science and planetary exploration are the subject of past studies [2,6,7]. One of these concepts, developed by NASA, focuses on the development a large solar sail for chasing comet Halley. This study was carried out at the Jet Propulsion Laboratory in 1977 and considered an 800×800 m solar sail for an 850 kg payload/bus [2,6]. A partly spin-stabilized and self-supporting 76×76 m square sailcraft, based on inflatable rigidizable booms, was proposed for the New Millennium Program Space Technology 5 (ST5) Geostorm warning mission, which would provide real-time monitoring of solar wind conditions [8]. The sailcraft would operate from the $L1$ point of the sun–Earth system toward the sun and offer increased warning time for geomagnetic storms, in contrast to an Earth-orbiting system. The concept of articulating a 2-axis gimbaled control boom was investigated for a 40×40 m square sailcraft proposed for the New Millennium Program Space Technology 7 (ST7) sail flight validation experiment [8]. This mission, with a gimballed control scheme (with thrust vector control), is detailed by Wie [8] with other control concepts, spin stabilization, control vane, and sailcraft using translating and/or tilting sail panels. Leipold et al. [9] present part of the European perspective in solar sail design. Kayser Threde and DLR, Germany Aerospace Center, have demonstrated a number of key technologies for solar sails. A 20 m sail deployment has been achieved using carbon-fiber-reinforced-polymer (CFRP) booms developed by DLR [9]. Other interesting concepts that employ solar sails include the Solar Polar Orbiter (SPO) and the Solar Power Imager. These concepts consider placing a sailcraft close to the sun to acquire enhanced solar measurements [10–14]. Observations directly over the solar poles are crucial to increasing our understanding of the sun. Most previous missions to study the sun have been restricted to observations from within the ecliptic. Solar sail missions orbiting the sun are envisioned to facilitate the development of a global three-dimensional picture of solar features and processes [10–14].

Because of the special characteristics of solar sails, sailcraft have been considered for long-duration spaceflight missions to the interstellar region [15–17]. Leipold et al. [15] details a study to develop an interstellar probe based on a solar sail platform to reach a distance of 200 AU in 25 years. After 6.5 years, the sail is ejected, having completed two photonic assist maneuvers around the sun. The spin-based platform, equipped with a highly integrated payload suite, operates autonomously to produce a 3-D mapping of the interstellar medium [15]. Wie [18] and McInnes [6] present a novel mission concept based on solar sails used to impact and deflect asteroids that can potentially collide with Earth.

Parallel to solar sail mission studies, past studies also focus on increasing the technological readiness level of solar sail technologies [9,13,19–22]. Sail deployment, boom technology, and attitude control are key technologies that have been demonstrated for near-term space missions [9,13,20–22]. Furthermore, ultralight micro solar sails have also been proposed based on flexible/inflatable structures for a GeoSail-type mission [19,23].

The goals of the GeoSail mission, defined by the ESA TRS study, consider engineering and scientific aspects. Among these, the engineering goals are the most stringent [2]. The present study assesses the engineering goals with respect to available technologies and proposes a realistic and robust design. The technology goals involve demonstrating the principle of solar sailing and extending the capability to other future solar sailing missions. The proposed design should demonstrate, in orbit, the principle of a solar sailing and generate observations and measurements of sail deployment and sail behavior. The sail should also demonstrate in situ sail jettison and measure sail–environment interaction. The scientific goals should investigate the occurrence of magnetic reconnection in the magnetotail plasma sheet and the reconnection processes at the subsolar point. Furthermore, the mission should also investigate the magnetosphere boundary layer [2,7]. The aim of the GeoSail study is to establish a cost-efficient and technologically feasible mission architecture for a solar sailing Earth magnetosphere exploration mission, with the main emphasis on the specific system design of the spacecraft and sail. Critical and mission-enhancing technologies are discussed.

Conventional geomagnetic tail missions require a spacecraft to be injected into a long elliptical orbit to explore the length of the geomagnetic tail. However, because the orbit is inertially fixed and the geomagnetic tail points along the sun–Earth line, the apse line of the orbit is precisely aligned with the geomagnetic tail only once every year. Approximately 3 months of data can be acquired, with only 1 month of accurate data from the tail axis. To artificially precess the apse line of the elliptical orbit and keep the spacecraft in the geomagnetic tail during the entire year would be prohibitive using chemical propulsion. A scientifically interesting 11×23 Earth-radii R_E elliptical orbit would require a ΔV on the order of 3.5 km/s per year of operation for apse-line rotation. A perigee at 11 Earth radii meets the bow shock, and an apogee at 23 Earth radii is optimum to

observe magnetic reconnection in situ. Although the ΔV for apse-line rotation is large, only a small acceleration continuously directed along the apse line is, in principle, necessary [3–5]. Because the precession of the apse line of the orbit is chosen to match that of the sun line, the sail normal can be directed along the sun line [2–7].

A. Mission Requirements

The GeoSail concept's main purpose is to demonstrate solar sailing as a feasible mission concept when doing research on plasma phenomena in the Earth's magnetosphere. The concept is compatible with ESA's Small Missions for Advanced Research in Technology (SMART) program, and emphasis is laid on a low-resource and low-cost design [1,2,7]. The solar sail is used to precess the apse line of the satellite orbit around the Earth, such that the orbit apogee and perigee remain continuously in the reconnection region in the magnetotail. Because of ΔV restrictions, missions using conventional propulsion systems can only remain in such a region for a limited time (about 3 months/year). By using a solar sail, a continuous presence of the orbit apogee and perigee in the reconnection regions can be accomplished without additional propellant. The concept of solar sailing has not yet been successfully demonstrated in space as a practical propulsion system for real space missions. The GeoSail concept is considered to be a strong contender for a solar sailing demonstration concept. The sail is jettisoned at the end of the mission or, in case of deployment failure, as a jettison demonstration. The successful demonstration of this concept is also crucial for future missions such as an SPO and Interstellar Heliopause Probe (IHP) [1,6,9–17]. Table 1 presents the GeoSail mission study requirements as specified by the ESA TRS design philosophy and ESA technology road maps [2]. A key goal of the study is to evaluate the feasibility of achieving the mission requirements or targets, such as solar sail mass or spacecraft bus mass, with near-term realistic technologies and to understand the technical shortcomings, which technologies need further development, and which near-term technologies can bring mass or performance benefits [2].

B. Science Objectives

The stated science objectives for GeoSail are to investigate 1) the occurrence of magnetic reconnection in the magnetotail plasma sheet, 2) reconnection processes at the subsolar point, and 3) the magnetospheric boundary layer. These regions and processes have been studied in the past and are the target of ESA's present 4-spacecraft Cluster mission. Additionally, NASA's forthcoming 4-spacecraft Magnetospheric Multi-Scale mission (2013 launch) is dedicated to the microphysics of reconnection, following the advances of Cluster. The launch of THEMIS (Time History of Events and Macroscale Interactions During Substorms) in 2007 has resulted in a multipoint analysis on the triggering and evolution of substorms, which is tightly linked to tail-reconnection processes. GeoSail's ability to maintain its apogee in the geotail against the natural precession relative to the sun–Earth line imposed by the Earth's orbital motion allows for the systematic study of the seasonal influences on the reconnection processes, especially in the geomagnetic tail. However, there are still undetermined science issues with the possible development of plasma bubbles that would be potentially created by the interaction of a solar sail with plasma in space [2,5,7,19]. Further analysis on the possible interference of the solar sail (shadowing, accuracy, and magnetic cleanliness) is necessary before the final payload suite is selected [2,7,24]. The strawman payload provides an excellent core suite of instruments that are suitable for both the primary mission objective (assessment of the sail performance and impact) and studying magnetic reconnection in the magnetosphere. Table 2 presents the strawman payload-suite characteristics for the GeoSail mission study [2].

C. Transfer Trajectory

Given the operational orbit ($11 \times 23\ R_E$) and considering the launcher requirement (Vega or a similar low-cost launcher), several possibilities exist to reach the final orbit.

1) With solar sail plus chemical propulsion (SS + CP), the transfer from the launcher injection orbit to the operational orbit is done with CP via high-thrust maneuvers.

2) With solar sail plus electric propulsion (SS + EP), EP provides the thrust during the multirevolution transfer.

3) With a dedicated solar sail (SS), no additional propulsion system (apart from the sail) is mounted and the SS provides the continuous thrust for the transfer. The selection of the best propulsion configuration requires the choice of the best tradeoff between the

Table 1 GeoSail mission study requirements

Primary objectives	Sail deployment demonstration in real space environment
Technology	Observation and measurements of sail dynamics
	Sail jettison and separation demonstration
	Measurement of effects of sail on space environment observations
	Ground-test model validation
Secondary objectives (science)	Understand how magnetic reconnection occurs in the magnetotail current plasma sheet
	Investigation of boundary layer, magnetic coupling, magnetospheric plasma waves, and plasma leaks through magnetopause
Payload	5 instruments
	Flux gate magnetometer
	Electrostatic analyzers
	Search-coil magnetometer
	Electric field instrument
	Solid-state telescope
Orbit and Launch	Apse-line control using solar sail
	Vega launch from Kourou in 2010
Orbit	11 $R_E \times 23\ R_E$ and $i = 23$ deg (ecliptic plane), where R_E is the Earth's radius
Operational lifetime	2 yr
	Spacecraft details
Total spacecraft mass (no sail)	87 kg
Sail mass	85 kg
	Sail details
Characteristic acceleration	0.1 mm/s^2
Size	43 m × 43 m (square)
Assembly loading	34 g/m^2 (final sail mass/sail area)
Material	TPEN film
Sail thickness	3.5 μm
Boom specification mass	34 g/m
Coating	Front: 0.1 μm Al, reflectivity 85%
	Back: 0.01 μm chromium, emissivity 64%

Table 2 GeoSail strawman payload-suite characteristics

Instrument	Units	Mass, kg
Fluxgate magnetometer (boom)	1	1.5
Electrostatic analyser	1	2.0
Solid-state telescope	1	1.0
Search-coil magnetometer (boom)	1	2.0
Electric field instrument	3	3.0
Data processing unit	1	3.0
Margin (20%)	——	2.5
Total	——	15.0

Table 4 Launch & transfer performances comparison

Performances	SS + CP	SS + EP
Launcher injection orbit	1500 km circular	3000 km circular
Initial mass	1500 kg	500 kg
Flight time	2.01 days (5 burns for apogee raising)	143 days
Propellant mass	1024.8 kg (5 burns for apogee raising) (2% gravity losses in perigee raising)	129.4 kg

three aforementioned possibilities. For a preliminary qualitative analysis, the main benefits and drawbacks of each configuration are summarized in Table 3. This analysis highlights mission architecture issues, possibilities to broaden the launcher spectrum, and backup possibilities for scientific return in case of possible failures.

The sail-only mission is inappropriate, because a deployment problem creates a single-point failure. Also, this particular scenario introduces the risk of solar sail degradation during the transfer phase. A preliminary estimation of the flight time of the sail transfer, considering the same sail designed for the operational orbit, is at least 3 times longer than the electric propulsion scenario (143 days) using two SMART-1-type engines (see Table 4). A launcher analysis is clearly required, because different possibilities arise, as detailed in Table 3. In addition, if the Vega (the nominal launcher) is not available, injection into higher-energy orbits is still possible via a Soyuz-2B launch from Kourou, and the flight time for multi-revolution transfers (SS and SS + EP) is reduced. If a piggyback launch into a higher-energy orbit is possible, such as an Ariane 5 launch into geosynchronous transfer orbit (GTO), the benefits of the electric propulsion become much more attractive, because the reduction in the transfer time is substantial.

1. *Propulsion Tradeoff*

The optimal transfer to operational orbit, in both electrical and chemical propulsion, must be analyzed for proper launcher and spacecraft (SC) architecture assessment. In the case of a Soyuz launch from Kourou, there is sufficient margin. However, for Vega, the launch margin fulfillment is more demanding, especially for the CP option. For transfer design, the baseline is a Vega launcher that injects the SC into a 23-deg-inclination circular orbit, and its performance is extrapolated for higher altitudes [25]. For the Soyuz case, the linear approximation/extrapolation for performance works well for 1000 to 4000 km circular orbits and is assumed to be feasible and compatible with the launch vehicle's user's manual [25].

According to [2], the total target mass into operational orbit is 172 kg (85 kg sail and 87 kg satellite bus), which is used as a design assumption. For the cases considered in this study (EP and CP), no perturbations are considered in the optimizations carried out. Thus, the central body is the only gravitational force assumed to act on the sail. In the EP scenario, certain assumptions are made based on existing EP technology and trajectory optimization techniques [26–28]. It is assumed that a continuous thrust is produced during eclipse periods, due to the limited number of restarts of electric engines, which imposes specific requirements on spacecraft batteries. A constant maximum thrust at 85.5 mN and specific impulse $I_{SP} = 1650$ s based on the SMART-1 Société Nationale d'Etude et de Construction de Moteurs d'Aviation (SNECMA) PPS-1350G thruster are used with a maximum power consumption of 1.1 kW [29]. For nominal operations, it is assumed that the EP thruster uses 85% of its maximum I_{SP} to have the additional capability of using the EP thruster if the sail deployment fails. An initial spacecraft mass (including the transfer module) of 500 kg is used, including a 20% margin, because of the additional transfer propellant and augmented dry mass, for which the propellant is 200 kg and the mass of engines, tanks, valves, pipes, and power control is estimated from SNECMA data to be 65 kg if 2 engines and 4 tanks are used (with only 1 engine, the transfer can still be carried out, but with an approximately doubled flight time).

In the CP hypothesis, similar design assumptions are made based on typical chemical thrust scenario, such as in other Earth-escape trajectory analyses [28]. An EADS Astrium 400 N bipropellant thruster is used (model S400-2), which provides a 400 N thrust at 318 s I_{sp}. For a 2-impulse transfer, the gravity losses with standard operational steering are high, making the scenario unfeasible. One solution is to split the apogee raising into several burns and perform an optimization of each burn duration and location using an explicit steering law for the thrust direction. Another solution is to use only one burn for each apse-raising maneuver and an implicit guidance logic (optimal control formulation) for the thrust direction. Although this proposed guidance scheme provides slightly better results than the explicit steering law, it is usually discarded due to operational complexity [30].

Table 3 Propulsion tradeoff for GeoSail transfer phase

SS + CP	SS + EP	SS
	Advantages	
Shortest flight time	Redundancy for Scientific return (EP module may be used for operational orbit maintenance if sail failure)	Lowest mass because an additional propulsion module is not required
Lowest operational costs	Higher launch mass margin	No consumables (propellantless)
Some science return if sail fails	Smaller and cheaper launcher possible, e.g., Dnper-1, or launch as piggyback (into GTO for instance)	Smaller and cheaper launcher possible, e.g., Dnper-1, or launch as piggyback (into GTO for instance)
Simplified sail operation	Simplified sail operation	
	Disadvantages	
Largest launch mass	Several months of flight time	Largest flight time (~3times the EP transfer time)
Additional upper stage	Longer radiation dose than CP (multiple crossing of Van Allen belts)	Longest exposition of SC to radiation dose and particle degradation
Low scientific return in case of sail failure (no precession of line of apsides)	Larger solar panels due to EP high power requirement and longer time in radiation belts	High degradation of sail due to long flight time (radiation belts, particles)
		Complete loss of mission in case of deployment failure
		Increased risk of collision with low-Earth-orbiting objects during the transfer phase

In an impulsive transfer, the alignment of the line of apsides with the sun–Earth line is not a complex issue. However, in the EP case, a guidance algorithm is required to achieve the required final orientation of the apse line. This is similar to the guidance algorithm used for the phasing for a rendezvous with a spacecraft such as that required in the ConeXpress mission [27]. This orientation of the line of apsides is neglected in the optimization, because the effect of the perturbations and the corrections to align the line of apsides is expected to have a small effect in the flight time and hence in the propellant mass. Another important design issue is that alignment of the apse line and sun line means thrusting in shadow, which impacts battery mass and subsequently increases the total system mass. Although the relative orientation can be neglected for trajectory optimization, it cannot be neglected for system design. The optimal solution for the GeoSail mission would be to thrust while the eclipse duration is below the battery capacity limit and to switch off thrusting during eclipse when it is above this limit. This strategy has a small impact on the transfer, because the larger eclipse periods take place at the end of the transfer, when the apogee has almost reached its operational value. This occurs, for example, in the last revolutions of the transfer, when the semimajor axis is higher and the variations in the orbital elements are the fastest (highest efficiency of the thrust).

The main characteristics of the considered transfers are presented in Table 4, in which the final mass includes the tanks and thrusters (or the additional kick stage) required to perform the maneuvers. The multiburn optimal explicit steering logic is used for the CP transfer design presented in Fig. 1, and the effect of the multiple burns in the final mass before perigee raising is depicted in Fig. 2. The EP optimal transfer (minimum time with continuous thrust) is presented in Figs. 3 and 4 and shows the most significant orbital parameters. Initially, the optimal control logic is focused on increasing the semimajor axis, and after a certain point, the control mainly aims to decrease the eccentricity. The cost function (flight time) has low sensitivity to the position of the optimization nodes (within a certain domain).

2. *Propellant Budget*

For the orbit perturbation analysis during the transfer, a separation is applied between deterministic perturbations (third bodies, solar radiation pressure, and nonsphericity of Earth gravity potential) and stochastic perturbations (launcher dispersion, navigation accuracy, and thrust uncertainties). Table 5 presents an estimation of the propellant mass budget for the two propulsion transfer options. For the EP transfer, a guidance algorithm previously developed is used, which compensates for the deviations from the optimal trajectory [26,27]. The simulations show negligible propellant mass penalty (less than 1 kg) due to the deterministic perturbations. Even if the orientation of the apse line is not considered, the low sensitivity of the flight time to the secular trajectory nodes indicates that the deterministic perturbations are not a big issue for EP. For the stochastic perturbations, the worst case is assumed, using a 10%-decreased thrust magnitude. The sensitivity to the launcher injection orbit is very small. The propellant mass for orbit maintenance during 2 years (nominal scientific mission duration) in the EP case is estimated by assuming a continuous thrust oriented in the line of apsides [i.e., only argument of perigee control and the transfer final mass (Table 5) without the sail mass (85 kg)]; that is, the orbit maintenance is performed by EP only if a sail deployment failure occurs and after jettison of a hypothetical failed sail.

In the chemical-propulsion scenario, the deterministic perturbations have a reduced effect due to the short transfer time and can be

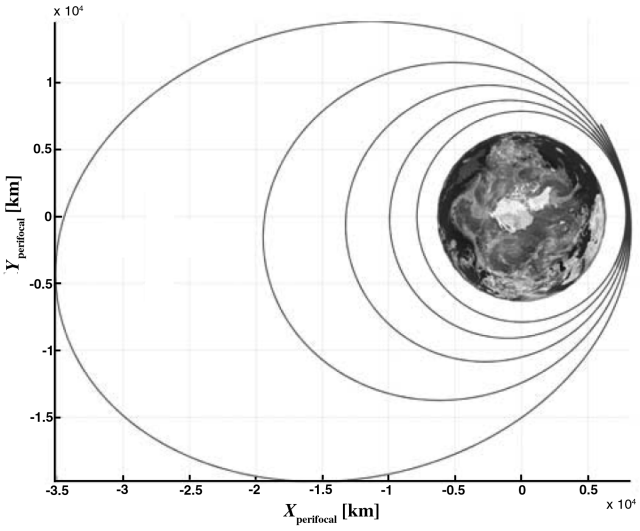

Fig. 1 Multiburn transfer with CP.

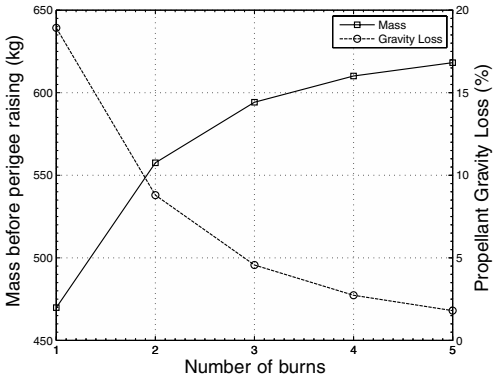

Fig. 2 Optimal gravity losses in the apogee raising as a function of the number of burns.

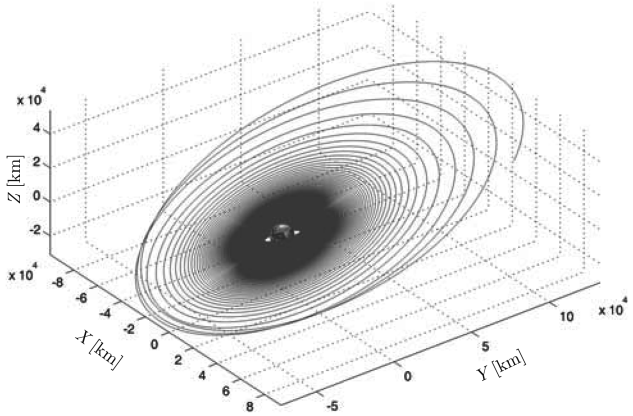

Fig. 3 Minimum-time transfer with EP.

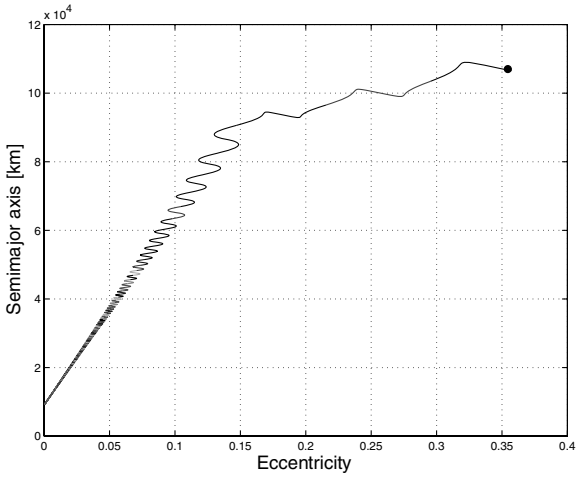

Fig. 4 Semimajor axis/eccentricity variation during transfer with EP propellant budget.

Table 5 Preliminary propellant budget

Propellant budget	SS + CP	SS + EP
Nominal transfer	1030 kg	129.4 kg
Deterministic perturbations	<10 kg	<1 kg
Stochastic perturbations (5%)	51.5 kg	14.4 kg
Orbit maintenance	286.5 kg	106.9 kg
Total propellant mass	1368 kg	250.7 kg
Final mass into orbit	132 kg	249.3 kg

included in the nominal transfer design and launch injection orbit. Therefore, a negligible contribution is expected to the overall propellant or ΔV budget. The stochastic perturbations can have significant effects, especially during the burn periods (attitude control and burn switch-on and switch-off times). Nevertheless, in a multiburn scenario, there is always the possibility to cancel undesired effects in subsequent burns and hence the number of trajectory correction maneuvers can be limited to just the final orbit adjustment. For this preliminary design, a margin philosophy of 5% is applied. The orbit maintenance for 2 years is computed by assuming an optimal 2-impulse strategy, because for the required eccentricity, the single impulse strategy is not optimal. The line of apsides oscillates and the scientific return degradation may be significant. A bipropellant thruster with a 340 s specific impulse is used. The orbit mass is the transfer final mass (see Table 5) excluding the sail mass (85 kg). For both the chemical and electrical options, two assumptions regarding the sail jettison and the decommissioning strategy have been considered:

1) No ΔV is provisioned for the jettison of the sail, because a mechanism is assumed to separate the SC and the sail. The solar pressure differential acceleration prevents a further collision. If a small ΔV ($\sim$1 cm/s) is required, the spacecraft thrusters and attitude control system (ACS) may be used.

2) For the decommissioning, no additional ΔV is envisaged in this preliminary analysis. However, the decommissioning should consider the probability of a possible jettison failure.

From the preceding results and analysis, the SS + EP mission presents more advantages than the SS + CP mission in terms of final mass into orbit ($\sim$100 kg), mission success probability, and launcher flexibility, provided that the operational and procurement costs are kept low by implementing the optimal onboard autonomy level and using mature technologies. Considering that the SS + EP is a more attractive option, electromagnetic contamination of instruments would need to be carefully assessed, although missions with similar payloads and propulsion systems to GeoSail, such as SMART-1, indicate no substantial issues with respect to instrument contamination from an EP system [29,31]. Therefore, the baseline design selected for the transfer phase of the mission is the SS + EP option. The corresponding model is based on SMART-1 propulsion heritage technology. Considering a 10% margin, the total mass, including structural parts and propellant, is 362 kg.

III. Solar Sail Trajectory

The GeoSail mission trajectory has been analyzed in [4,5] under the assumption of an ideal solar sail force model and including the effect caused by the Earth's shadow. Recently, a new enhanced steering law has been proposed in which the sail's behavior is characterized by an optical force model and shadowing effects due to the eclipse periods [32]. In the GeoSail mission, the solar sail is assumed to orbit within the ecliptic plane so that only three osculating orbital elements (semimajor axis a, eccentricity e, and argument of perigee ω) are required to describe the evolution of the trajectory. The sail normal $\hat{\boldsymbol{n}}$ is directed, by assumption, within the ecliptic plane so that there is only an in-plane acceleration due to the solar radiation pressure. To investigate steering laws for the apse-line precession, the following Lagrange planetary equation is employed [4]:

$$\frac{\mathrm{d}\omega}{\mathrm{d}t} = \frac{r^2}{\mu e}\left[-a_r \cos\nu + a_t\left(1 + \frac{r}{a(1-e^2)}\right)\sin\nu\right] \tag{1}$$

where a_r and a_t represent the radial and transverse components of the sail propulsive acceleration, r is the Earth-sail distance, μ is the Earth's gravitational parameter, and ν is the true anomaly. The orbit geometry is shown in Fig. 5, along with the sail pitch angle α and the ideal thrust orientation angle relative to the radial direction $\varphi = \pi - [\alpha + \nu - (\delta - \omega)]$.

The solar sail acceleration is introduced through an optical force model [32]: that is,

$$\boldsymbol{a} = f_s a_c \cos\alpha[b_1\hat{\boldsymbol{r}}_\odot + (b_2\cos\alpha + b_3)\hat{\boldsymbol{n}}] \tag{2}$$

where b_1, b_2, and b_3 are the optical coefficients ($b_1 = b_3 = 0$ and $b_2 = 1$ for an ideal, perfectly reflecting, sail), a_c is the sail characteristic acceleration, and f_s is the shadow function: that is $f_s = 0, f_s = 1$, or $0 < f_s < 1$, according to whether the solar sail is in umbra, in sunlight, or in penumbra, respectively. A conical shadow model is assumed in all of the simulations. Note that for the rotation of the apse line to be synchronous with the rotation of the sun line, the identity $\dot{\omega} = \dot{\delta}$ must hold, where $\dot{\delta} \triangleq 0.9856$ deg/day. The developed optimal steering law allows one to suitably trade off between the conflicting requirements of maximizing the apse-line precession capability and the control effort required to achieve that precession. In mathematical terms, the problem can be presented as that of maximizing the functional J, defined as

$$J = \eta\omega_f + \frac{(1-\eta)}{2}\int_0^{2\pi}\cos^2\alpha\,\mathrm{d}\nu \tag{3}$$

where $\omega_f \triangleq \omega(t_f)$ and subscript f stands for final (that is, after a whole orbital period). The tradeoff between sail precession effectiveness and control effort is accomplished through the value of parameter $\eta \in [0, 1]$. Values of η close to 0 correspond to small variations allowed for the pitch angle, whereas, as long as η is increased, more control energy may be employed, thus increasing the solar sail precession efficiency. Figure 6 shows the sail performance as a function of η for different values of dimensionless characteristic acceleration $a_c/a_{c_{\mathrm{des}}}$, where $a_{c_{\mathrm{des}}} \triangleq 0.096$ mm/s^2 corresponds to the design value of the characteristic acceleration in [2]. Actually, the dimensionless apse-line precession rate $\dot{\omega}/\dot{\delta}$ depends on η, even if this dependence is quite moderate. In fact, it can be shown (see [32]) that there exists a linear relationship between $\dot{\omega}/\dot{\delta}$ and the solar sail characteristic acceleration. To guarantee that the GeoSail orbit is sun-synchronous, the condition $\dot{\omega}/\dot{\delta} = 1$ must be satisfied. Assuming $\eta = 1$ (i.e., a control law that maximizes the apse-line rotation), the minimum admissible value of the characteristic acceleration is

$$a_c = 1.1\,a_{c_{\mathrm{des}}} = 0.106 \text{ mm/s}^2$$

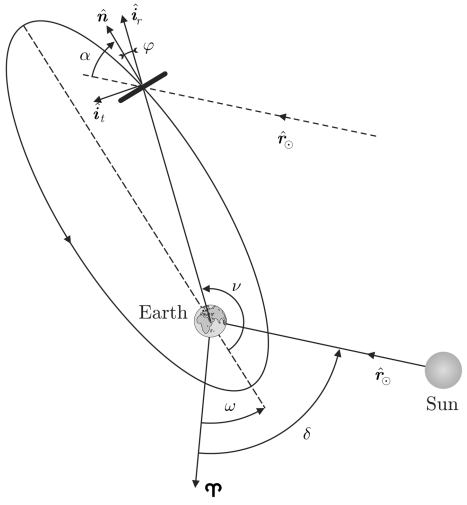

Fig. 5 GeoSail orbit geometry.

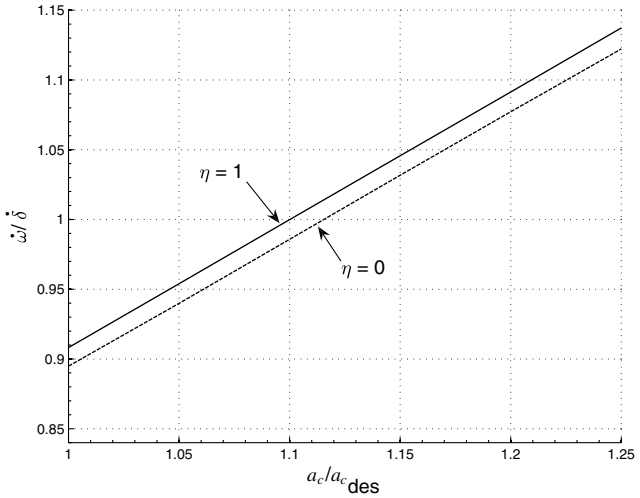

Fig. 6 Sail performance as a function of dimensionless characteristic acceleration.

IV. Solar Sail Design

The emphasis for solar sail design is mainly to successfully deploy the maximum effective sail area with the lowest possible mass. Improvements in this context aim to carry larger payloads, to enable higher acceleration for long-term missions, and to keep the sailcraft inertia at a minimum for attitude maneuvers and structural stability. Design options exist in many technological areas for a solar sail design: material selection, storage, and deployment technologies. There has been a recent emphasis on the development of many of the key sail technologies based on various boom/deployment technologies, including deployment of solar sail designs in large vacuum facilities [13,20,21,33–35].

A major issue in solar sail design is the development and deployment of lightweight, rigid, long structural booms. They affect the sail performance in two ways: 1) directly with the mass of the booms themselves and 2) indirectly with the mass and size of the related sail deployment and storage facilities. The proposed GeoSail design is based on the IOB design, which provides an advantageous solution for both sail-boom requirements [33]. Commonly known technologies for deployable booms with a reasonable stiffness-to-mass ratio are limited in length, due to inherent stresses that define the necessary storage volume. The IOB technology uses similar boom cross sections, but shifts the assembling process into orbit. The storage of two semifinished half-sections allows compact storage, which is a critical design feature for solar sails. During deployment, the boom halves are to be aligned to each other and adhesively bonded. With the possibility of varying shell thickness or size of the cross section, a design close to the load conditions becomes feasible. This optimizes the structure with respect to the mass requirements. Considering that the sail deployment is a one-shot process, the majority of the associated mechanical and structural components are not needed afterward. The IOB sail design allows jettisoning of this mass fraction after reaching its desired size, thus substantially reducing the sail mass [33].

The feasibility of the IOB concept has been built in the form of a breadboard model aimed for on-ground technology demonstration and tests with the prospect of near-term flight-model development. The demonstrator, as depicted in Fig. 7, consists of three main sections in the feeding line of the carbon-fiber-reinforced polymer segments: a storage unit, a drive unit, and an alignment unit. Despite the high mass of the breadboard model (25 kg), the choice made for the on-ground demonstration of a reduction in the range of at least 50–75% is feasible for flight models [33]. To demonstrate the possibility of jettisoning a large fraction of total mass, the storage unit is designed to separate from the main sail structure, a feature that is not necessarily available with other sail deployment systems [33]. A solar sail design that incorporates the capability to eject the deployment structure, subsequently reducing the mass of the sail, is

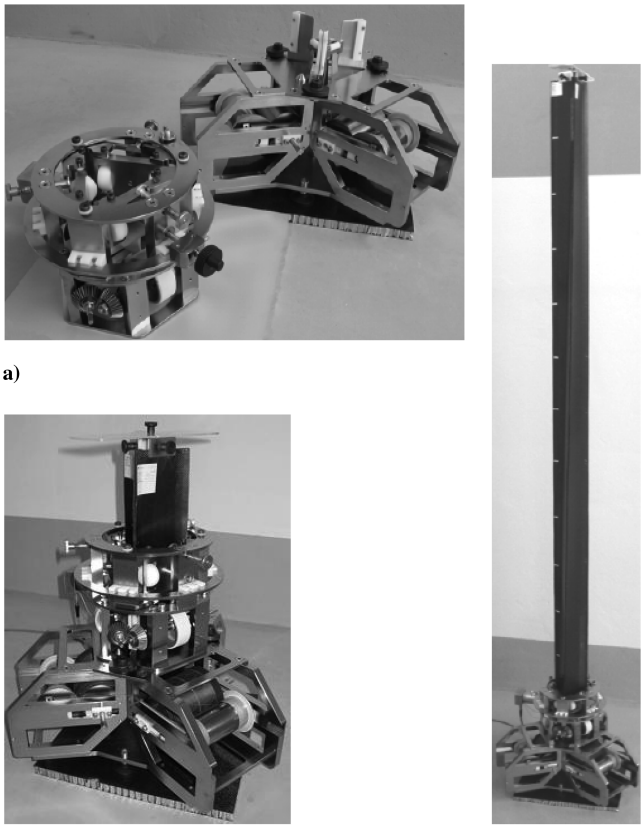

a) **b)** **c)**

Fig. 7 IOB breadboard deployment module: a) separated in fixed and ejectable parts, b) launch mode, and c) deployed.

the L'Garde sail. The design was recently tested at the NASA Space Power Facility at Plum Brook Station, Ohio [13,21,35]. The storage unit includes three equal compartments with storage and a spring-loaded pressure roll. The unwound segments (still separated by sheet-metal plates) are led into plastic guiding elements. A speed-controlled 24 V dc drive motor feeds the segments by friction wheels. All three feeding lines are connected and equalized by a bevel gear. The sail film is then held by the three-corner method, which has been previously tested [9,33].

A. GeoSail Sail Design and Tradeoff

In most references in the literature [2–16], there is limited information on the sail design and the design methodology that was followed. Most studies have used existing solar sail technical information or projections to get an estimate on the sail mass and performance properties. In this paper, three sail configurations are considered for the GeoSail solar sail design and tradeoff:

1) Configuration A is a 3-boom triangular shape.

2) Configuration B is a square 4-boom shape.

3) Configuration C is a square 4-boom shape with a 10×10 m cutout in the center for payload field-of-view purposes (Fig. 8).

Table 6 presents the solar sail design requirements for the GeoSail mission as specified by the ESA TRS literature [2]. Table 7 shows the preliminary results from the design and tradeoff for different sail shapes (configurations A–C). The bending force, sail technology availability on sail technology (IOB booms and CP-1 film), and GeoSail requirements [2] form the basis of the sail sizing. The main conclusion from the preliminary tradeoff is that the 3-boom triangular shape requires a higher structural rigidity than configurations B and C; however, it comes with the smallest mass, as depicted in Tables 8 and 9. The boom stiffness affects the film tensioning, an aspect that is not considered in the present study. The booms for the 3-boom configuration are heavier, for support purposes. The satellite bus mass is fixed to 85 kg for the sail sizing.

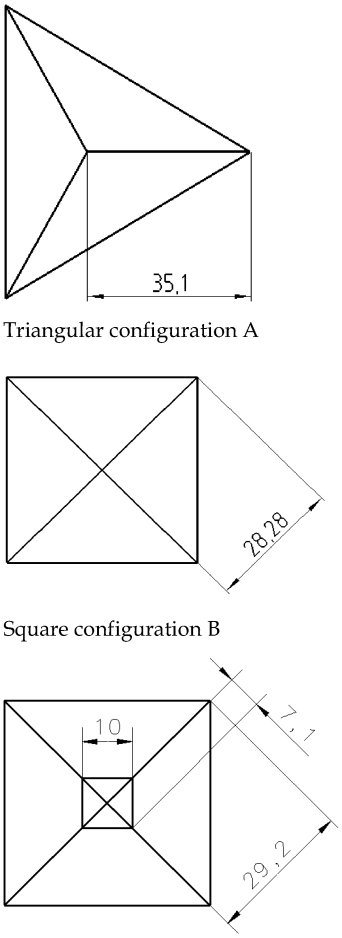

Triangular configuration A

Square configuration B

Square configuration C with internal cutout

Fig. 8 GeoSail configuration tradeoff.

Table 9 provides a summary of the three sail configurations analyzed. The ejectable unit for the sail design is the same for all configurations. The boom mass savings for the square sail are slightly larger than the savings obtained from employing fewer components for the sail deployment using the 3-boom configuration A. Larger-sailcraft missions, such as the solar orbiter and IHP, are expected to exhibit a similar, but amplified, trend. Configuration C is the heaviest in mass by a small margin and has the 10 m center cutout. Option B is selected due to its simpler design (without the cutout); however, design C should also be further analyzed to ensure that payloads have a continuous and clear field of view.

V. Attitude Control System

In theory, the orientation of large solar sails may be controlled through the combined use of attitude determination techniques and control systems that are typically employed in small satellites.

Table 6 GeoSail design requirements

Parameter	Symbol	Value	Units
Solar radiation pressure	P	4.56×10^6	N/m^2
Sail efficiency	η_s	1.85	——
Mass solar sail structure	m_S	TBD	kg
Total S/C (bus) mass	m_T	85	kg
Sail area	A	1600	m^2
Solar sail loading	s	53.125	g/m^2
Characteristic acceleration	a_0	0.10	mm/s^2
Traveling distance	s	49,725,965	km (0.33 AU)

However, for an 85 kg sailcraft, small reaction wheels and a conventional propulsion subsystem with a limited amount of propellant may be inadequate, impractical, or even undesirable. In particular, the large moments of inertia, its large solar-pressure-imbalance disturbance torque, and its extended sailing voyages render these classical techniques impractical for the present application.

One method of actively controlling the attitude of a 3-axis stabilized sailcraft is to change its center-of-mass location relative to its center-of-pressure location. This can be achieved by articulating a control boom with a tip-mounted payload/bus [8,22]. Although the essential idea behind the c.m.–c.p. methods that are traditionally used for solar sails is simple, there are various practical implementation issues. Furthermore, these various attitude control approaches introduce their own advantages and disadvantages in terms of pointing accuracy, controllability, stability, and other system-level tradeoff issues (e.g., mass, power, volume, and cost). The selection of a particular attitude control approach for a specific mission requires detailed system-level tradeoffs [8,13,15,18,19,22].

There is a need to develop an efficient scalable ACS with the optional possibility of decoupling the ACS from the sail booms, adding design flexibility and simplicity to the sail design. The design proposed for GeoSail is a spacecraft-bus-oriented ACS system decoupled from the sail, as depicted in Fig. 9. Although challenging due to the large and persistent SRP disturbance leading to excessive angular momentum buildup, the proposed ACS system illustrated in Fig. 10 enables a compact and robust control scheme using flight-proven technologies with minimum risk and scalability.

A trim-ballast system based on four 10 m booms with 2 kg ballast masses is used to trim the sail and allow attitude control with microreaction wheels (Fig. 10). The booms are also used to place the miniature pulsed plasma thrusters (PPTs). The large torque arms are used to maximize the effectiveness of the small forces produced by the PPTs. Roll control cannot be achieved through the trim-ballast system, because it is a 2-axis control system (pitch/yaw), or by the bus microthrusters/reaction wheels, as the torque they can produce is small. The roll SRP disturbance that is considered as half of the pitch/yaw disturbance creates a pinwheel disturbance torque and an excessive angular momentum, which need to be compensated by some means of actuation. An SRP force of 0.01 N generates disturbance torques of 1 $mN \cdot m$ about the pitch/yaw axes and 0.5 $mN \cdot m$ about the roll axis, leading to an angular momentum buildup of $31,536\ N \cdot m \cdot s$ for the 2-year GeoSail mission. Compensating for this excessive angular momentum buildup, large amounts of propellant would be required, reaching levels of 30 kg, a mass overhead that is not compatible with the small-satellite bus design. However, if the thrusters are placed on four 10 m booms, the large lever arms amplify the torque that is produced by the thrusters with minimum mass. The booms are also used to carry the 2 kg ballast masses for sail trimming [19]. Another advantage of the boom mounted PPTs is that they can be used in case of attitude failure to place the sail in a safe pure-spin mode. Figure 11 presents the trim-ballast control system [22]. Figure 12 illustrates the feasibility of counteracting solar disturbance torques (0.5 $mN \cdot m$) using the bus-based booms/PPT scheme with moving masses. The simulation employs parameters and properties listed in Table 10. Figure 12 also depicts the PPT firings needed for roll control of the sail for a 20 deg roll reorientation maneuver and the realistic performance of the proposed trim balance system, which only requires a maximum 10 m length. It is also evident from Fig. 12 that the trim-ballast rates are feasible with existing miniature-motor technologies.

VI. Spacecraft Bus

The core structure is a standard Surrey small-satellite modular self-supporting stack of equipment boxes. Each module box carries one or more subsystems, serving as both subsystem enclosure and structural element. The top facet is the interface with the solar sail module. This is surrounded by shear panels that connect and transfer the loads from the stack to the facet and to which nonstructural ministacks of nanotrays are bolted. These nanotrays represent the

Table 7 Tradeoff and sail design for the GeoSail mission

Solar Sail Parameters	Symbol	Configuration A	Configuration B	Configuration C	Units
Sail area	A	1600	1600	1600	m^2
Boom length	l_b	35.10	28.28	29.2	m
SRP	P	4.56E − 06	4.56E − 06	4.56E − 06	N/m^2
Sail efficiency	η	1.85	1.85	1.85	——
Total force	F_t	1.35E − 02	1.35E − 02	1.35E − 02	N
Boom tip bending force	$F_b = 2/9(F_t)$	3.00E − 03	2.25E − 03	1.69E − 03	N
Maximum distance/neutral line	$t/2$	0.08	0.07	0.07	m
Allowable bending radius	$R = (t/2)/e$	16	14	14	m
Moment of inertia of the cross section	I	2.49E + 05	1.66E + 05	1.66E + 05	mm^4
Young's modulus	E	50,000	50,000	50,000	N/mm^2
Boom deflection	f	3.5	2.0	1.7	mm
Cross section	L	350	310	310	mm
Number of plies	——	3	3	3	——
Specific mass	$m_{\mathrm{CFRP}_{\mathrm{spec}}}$	65	65	65	g/m^2
Mass per length	$m_{\mathrm{CFRP}_{\mathrm{length}}}$	68.25	60.45	60.45	g/m
Volumetric fiber	——	55	55	55	%
Density of matrix material	——	2	2	2	g/m^3
Density of fiber material	——	1.7	1.7	1.7	g/m^3
Matrix mass	m_{matrix}	65.70	58.2	58.2	g
Boom weight per length	m_{spec}	133.95	118.64	118.64	g/m
Boom structure mass	m_{struc}	14102.54	13422.26	13835.35	g
Boom shell thickness	——	0.35	0.35	0.35	mm
Allowable strain	e	0.005	0.005	0.005	——
Bending radius	——	35.00	35.00	35.00	mm
Blanket substrate density	ρ	1434	1434	1434	kg/m^3
Thickness (CR1–0.25 mil)	t_{CR1}	6.35E − 06	6.35E − 06	6.35E − 06	m
Specific film mass	——	9.11	9.11	9.11	g/m^2
Film mass	m_f	14569	14569	14569	g

Table 8 Sail deployment parameters

Sail deployment parameters	Symbol	Configuration A	Configuration B	Configuration C	Units
Boom length	l_b	35.10	28.28	29.15	m
Boom weight per length	m_{spec}	133.95	118.64	118.64	g/m
Boom structure mass	m_{struc}	14.10	13.42	13.84	kg
Sail area	——	1600	1600	1600	m^2
Sail area/boom size	——	45.6	56.6	54.9	m
Film mass	——	14.6	14.6	14.6	kg

Table 9 Total mass properties for the GeoSail sailcraft configurations

Layout configuration			Configuration A		Configuration B		Configuration C
Component	Mass, kg	Units	Total mass, kg	Units	Total mass, kg	Units	Total mass, kg
Sail mass	——	——	14.6	——	14.6	——	14.6
Boom mass	——	——	14.1	——	13.4	——	13.8
End fittings	0.1	3	0.3	4	0.4	4	0.4
Main frame	——	——	10.0	——	10.0	——	10.0
Guiding unit	1.5	3	4.5	4	6.0	4	6.0
Ejectable frame	——	——	10.0	——	10.0	——	10.0
Sail container	——	——	6.0	——	6.0	——	6.0
Ejection unit	——	——	2.0	——	2.0	——	2.0
Storage drum	0.65	3	1.95	4	2.6	4	2.6
Tape removal	0.35	2	0.7	2	0.7	2	0.7
Driving unit	1.5	3	4.5	4	6.0	4	6.0
Launch mass	——	——	68.6	——	71.7	——	72.1
Mass after jettisoning	——	——	43.5	——	44.4	——	44.8

next step in miniaturization and are a direct result of the work done on developing smaller, more efficient, subsystems, demonstrated on the SNAP-1 (Surrey Nanosatellite Applications Program) nanosatellite. The GeoSail mission does not pose a substantial challenge for the structure design. Thus, a standard small-satellite structure is used, as illustrated in Fig. 13 [36].

The S-band RF system consists of two transmitters and receivers with associated antennas. The transmitters are cold-redundant and have their own default frequency allocation at startup, and so they can work autonomously. The setup has omnidirectional coverage and includes provisions for safety and backdoor commanding for emergency operations. The S-band system includes two 9.6 kbps CP frequency-shift-keying receivers and two 2 Mbps biphase-shift-keying transmitters.

The data handling system is based on two heritage computers, with a third redundant computer that is an upgrade from the heritage computer. This allows for redundancy and high performance while preserving heritage. The onboard data handling (OBDH) is divided into platform and payload sides, each with its own dual-redundant controller-area-network buses. A high-speed bus is provided

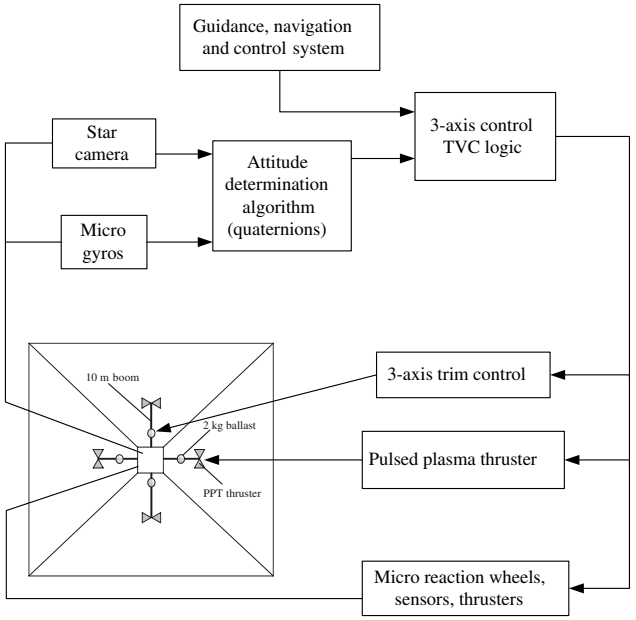

Fig. 9 Solar sail bus attitude control system architecture (TVC denotes thrust vector control).

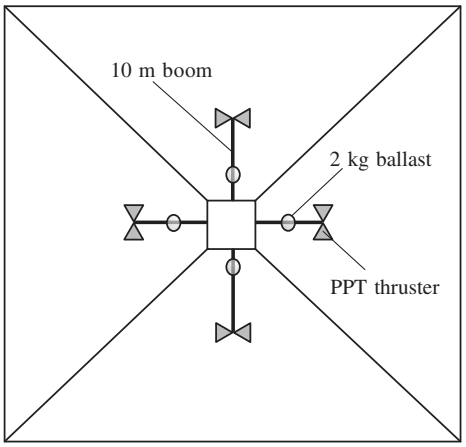

Fig. 10 Satellite bus ACS for GeoSail.

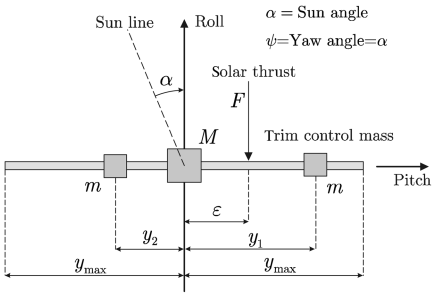

Fig. 11 Trim-ballast control system [19].

between the redundant processor module and the two data recorders. The main goal of the platform side is to do attitude control, and the payload side handles spacecraft housekeeping. Data is stored in synchronous dynamic RAM devices. Configuration via the onboard processor provides a means of controlling storage. This includes a mode that provides protection of captured data against single-event upset. These devices (hardware data recorders) are based on recent small-satellite technologies based on previous solid-state data recorders units, one of which is provided for additional backup [36].

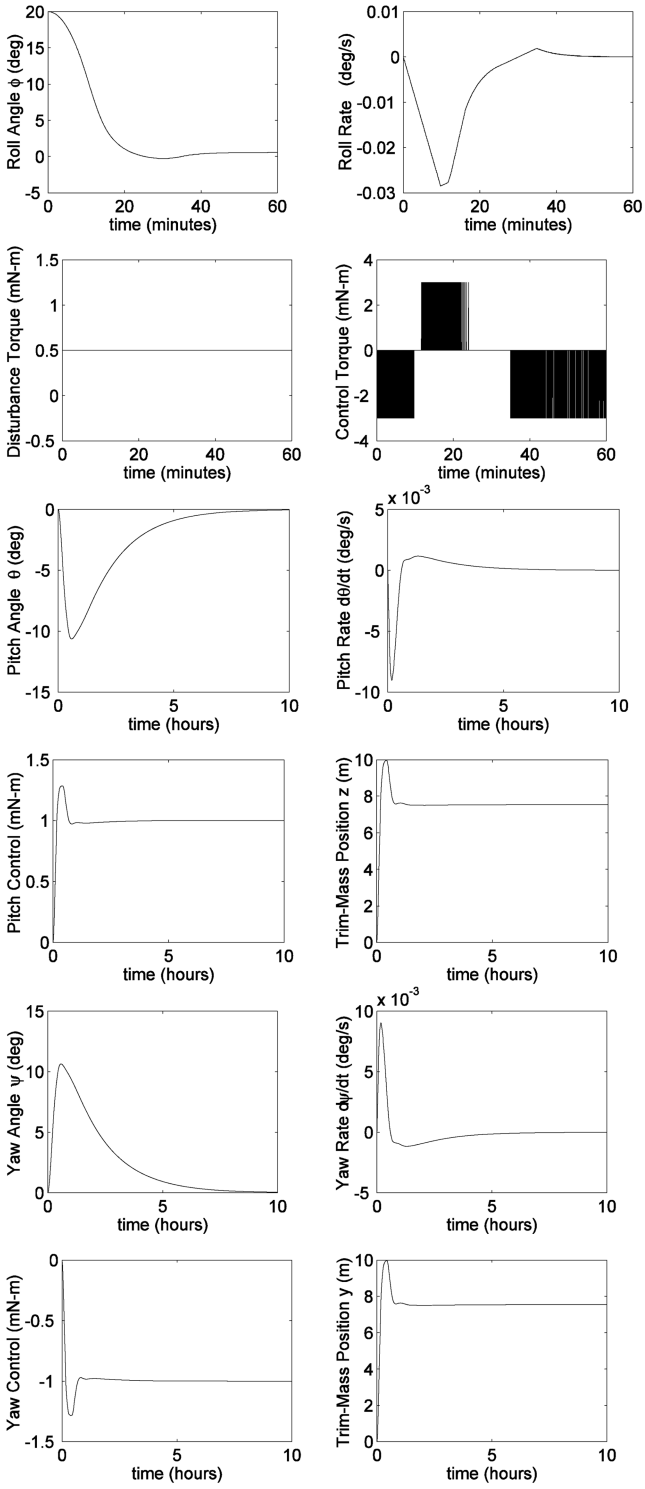

Fig. 12 Sail bus ACS SRP disturbance simulation.

The GeoSail bus power system uses heritage from previous Surrey spacecraft power systems (mainly, the DMC-1 spacecraft). The power system uses a battery bus topology and delivers an unregulated 28 V bus to the platform and payloads. The solar arrays are connected to the bus via battery charge regulators, providing a versatile and efficient method of maximizing panel power during sunlight by adapting to array characteristic variations with changing temperature. Direct connection between the battery and the bus ensures maximum efficiency during battery discharge in eclipse. The power system design is modular and can be scaled to meet varying power demands for different missions [36]. GaAs multijunction cell technology is used on the GeoSail solar arrays, and a lifetime of two

Table 10 Simulation parameters

Parameter	Value
$N_{\text{SRP-D}}$	$0.5\ \text{mN} \cdot \text{m}$
θ_e	20 deg
N_{control}	$3\ \text{mN} \cdot \text{m}$
M_{tip} (2 thrusters)	1 kg
I_i (total impulse)	$2000\ \text{N} \cdot \text{s}$
I_{TI} (total torque impulse)	$20,000\ \text{N} \cdot \text{m} \cdot \text{s}$

years was taken into account in the sizing of the solar panels, in addition to solar sail shadowing.

A. Propulsion

A low-mass and robust propulsion subsystem such as a xenon-based resistojet thruster system is needed for sail ACS recovery (backup) without contaminating the sail assembly. The propulsion system should potentially act as a backup for apse-line rotation in case the sail fails to avoid a total mission failure. The proposed propulsion system comes with added benefits. Gaseous propellants avoid any liquid sloshing effects and are stored in a miniature 2.1 liter propellant tank of titanium construction. The tank has a maximum expected operation pressure of 44 bar. The propulsion system is built as a module with an integrated thruster (resistojet xenon/neon), as depicted in Fig. 14 [37]. The thruster alignment can be modified at both the module and spacecraft levels. Bang–bang pressure regulation control allows the thrust level to be throttled between 10 and 50 mN [37]. The proposed xenon/neon propulsion system contains 6 microthrusters and, with a total mass of 10.3 kg, is a low-cost and compact subsystem designed for orbit control and for backup attitude control. Table 11 presents the propulsion-system characteristics.

Table 11 GeoSail propulsion-system characteristics

Parameters	Value
Propellant Xe/Ne	500 g/176 g
Thrust	20–50 mN
Specific impulse	42 s/100 s at 300°C
Total impulse	380 Ns
System volume	2.1 liter
Lifetime	2 yr
Power	19 W peak, 0.6 W idle
Dry mass	6.72 kg
Dimensions	$400 \times 254 \times 215$

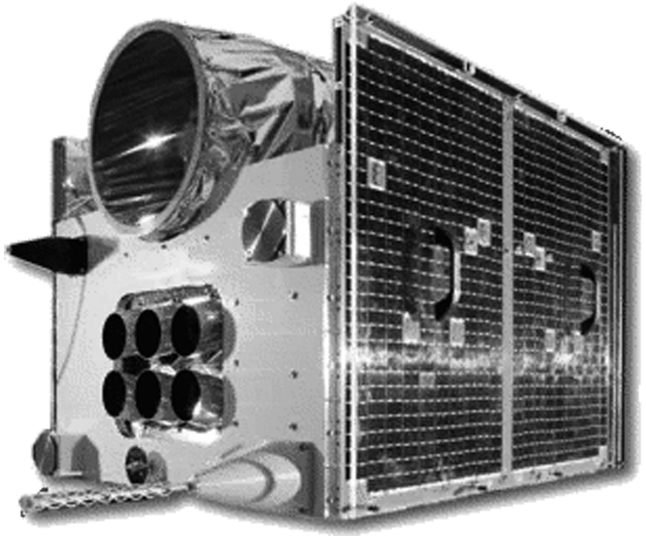

Fig. 13 Surrey small-satellite modular bus platforms.

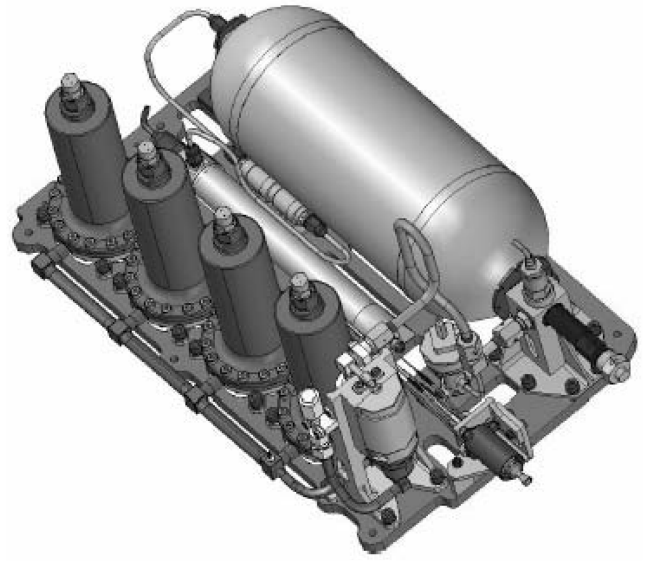

Fig. 14 GeoSail bus propulsion system.

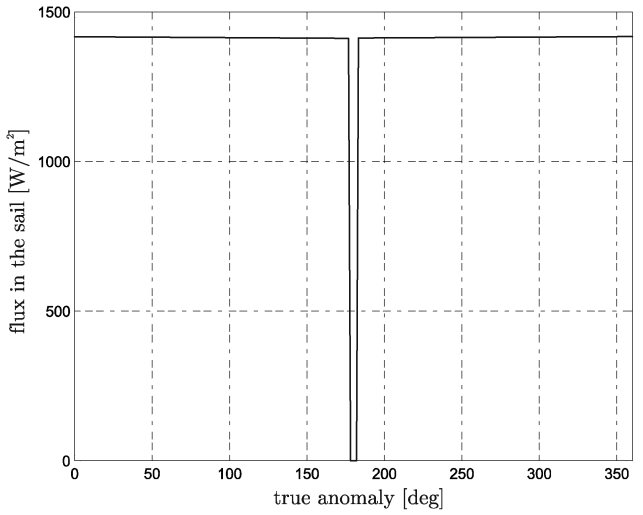

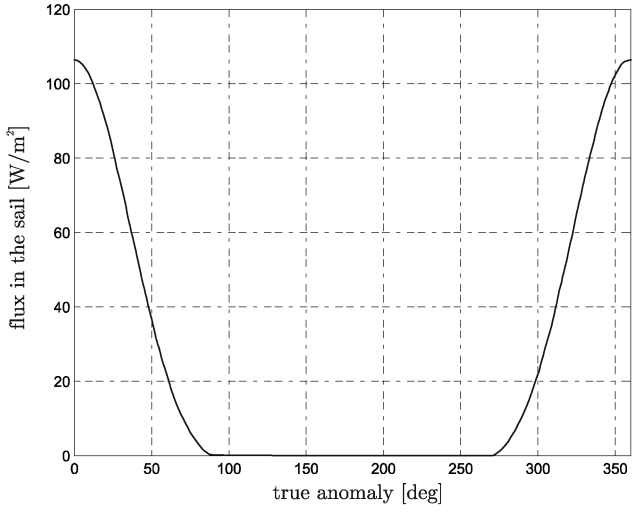

Fig. 15 Incident flux through one revolution in both sides of the sail.

Table 12 GeoSail bus mass and power breakdown

Subsystem	Mass, kg	Average power, W	Peak, W
Payload	15	3	5
AOCS	23	12	18
Propulsion	10.3	22	35
OBDH/harness	7	5	7
RF	4	4	8
Thermal	3	4	4
Power	6	1	3
Structure	9	——	——
Margin (10%)	7.73	5.1	8
Total mass	85	56.1	88

B. Thermal Design

The orbit of GeoSail is defined by its perigee, always located on the sun–Earth line, and so the synodic frame centered at the Earth is chosen. In this system, the spacecraft follows a non-Keplerian orbit, for which the perigee is located on the negative part of the x axis at a distance of 11 R_E and the apogee is located along the positive part of the x axis at 23 R_E. The most constrained point is considered to be at the epoch, in which the Earth is located at perihelion. During that epoch, the two relevant points for the spacecraft are the perigee and the apogee, for which the radiation flux is at a maximum or minimum. The orientation of the sail is considered to be always pointing toward the sun, because it is the selected steering law for apse-line precession while maintaining orbit shape and energy. This orientation gives two possible faces to analyze: one pointing toward the sun and the other pointing in the antisun direction.

The solar flux received in the face oriented to the sun shows small variation (due to albedo and distance to the sun variation), except near the apogee, when the SC enters in the umbra cone of the Earth, as illustrated in Fig. 15. There, the radiation received by the sail from the solar flux is zero. The infrared flux is 6 orders of magnitude lower than the direct sun illumination, due to the far distance from the Earth. For the face pointing in the antisun direction, the greater contribution comes from the albedo radiation. It reaches the maximum at the perigee and decreases to reach the minimum at true anomaly of 90 deg, which corresponds with the sail perpendicular to the sun–Earth direction.

C. Spacecraft Bus Mass and Power Breakdown

Table 12 shows a summary of the mass and power breakdown of the GeoSail bus design. A fixed 10% margin is used, compatible with the ESA TRS margin philosophy [1,2]. The recommended 15 kg payload is used, which includes a part (50%) of the solar-sail-monitoring package (imaging payload); the other 50% is sensors that are included on the sail booms. The attitude and orbital control system (AOCS) dominates the design of the structure (based on a standard microsatellite bus) and of a propulsion system for backup ACS capability and for limited apse-line control in case of sail failure. The bus includes some active thermal design components for the long eclipse intervals, and the power budget is compatible with traditional small-satellite designs; margins of 10% are used because all satellite bus subsystems are based on current technologies and small-satellite heritage. The 10% mass and power margin is in agreement with the ESA TRS margin philosophy [2].

VII. Conclusions

GeoSail is proposed as a low-cost solar sail mission to study the Earth's magnetotail. Because of ΔV restrictions, missions using conventional propulsion systems can only remain in the Earth's magnetotail region for a limited time (about 3 months/year). By using a solar sail, a continuous presence of the orbit apogee and perigee in the reconnection regions can be accomplished without additional propellant. Recent advances in solar sail design and small-satellite technology are employed in this study to provide a lighter and realistic alternate design for the GeoSail mission. The 15 kg payload contains a full suite of sensitive plasma detectors based on the recently launched THEMIS spacecraft constellation-payload design. Combinations of solar sail with electric and chemical propulsion are the basis of a tradeoff study that investigates the subsequent impact on spacecraft mass and the time of flight during the transfer to the reference orbit. Because of mass constraints, an electric propulsion design based on the SMART-1 architecture was selected as the baseline option, leading to a 362 kg mass design for the transfer vehicle. A new sail steering law that takes into consideration the sail degradation effects and eclipses is used to design the solar sail subsystem. For the sail design, the IOB technique is used to deploy efficiently lightweight rigidizable booms. The proposed design, which has been tested in laboratory experiments on the ground, comes with the inherent design feature of in-space jettison of all used and unnecessary components after sail deployment, thus significantly reducing mass. Different sail configurations and designs were traded off against each other, leading to a practical, realistic design with an after jettison mass of 44.4 kg. A bus-based ACS subsystem is proposed that combines a trim-ballast system with a PPT low-cost propulsion system used as backup, providing robust attitude control. The sail bus uses commercial, off-the-shelf, subsystems derived from small-satellite heritage, leading to significant mass savings for a 85 kg bus, with peak and average power requirements of 88 and 56.1 W, respectively: well within existing small capabilities.

Acknowledgments

The authors would like to thank the anonymous reviewers and the Associate Editor for the helpful suggestions that improved the quality of the paper.

References

[1] Falkner, P., Atzei, A. C., van den Berg, M. L., Renton, D., Schulz, R., and Sterken, V., "ESA Technology Reference Studies in the Context of Cosmic Vision 1525," *Geophysical Research Abstracts*, Vol. 8, 2006, Paper 07281.

[2] Science Payload and Advanced Concept Office, "Executive Summary of the GeoSail Study," ESA, Rept. SCI-A/2006/005/GS, Paris, Apr. 2006, ftp://ftp.rssd.esa.int/pub/pfalkner/GeoSail_TRS/%5BRD3%5D%20GS_exec_summary.pdf [retrieved 21 Nov. 2006].

[3] Macdonald, M., and McInnes, C. R., "GeoSail: an Enhanced Magnetospheric Mission Using a Small Low-Cost Solar Sail," 51st International Astronautical Federation Congress, Rio de Janeiro, International Astronautical Federation Paper IAF-00-W.1.06, Oct. 2000.

[4] McInnes, C. R., Macdonald, M., Angelopoulos, V., and Alexander, D., "GeoSail: Exploring the Geomagnetic Tail Using a Small Solar Sail," *Journal of Spacecraft and Rockets*, Vol. 38, No. 4, July–Aug. 2001, pp. 622–629. doi:10.2514/2.3727

[5] Macdonald, M., McInnes, C. R., Alexander, D., and Sandman, A., "GeoSail: Exploring the Magnetosphere Using a Low-Cost Solar Sail," *Acta Astronautica*, Vol. 59, Nos. 8–11, Oct.–Dec. 2006, pp. 757–767. doi:10.1016/j.actaastro.2005.07.023

[6] McInnes, C. R., *Solar Sailing: Technology, Dynamics and Mission Applications*, Springer Praxis, New York, 1999.

[7] Macdonald, M., Hughes, G., McInnes, C., Lyngvi, A., Falkner, P., and Atzei, A., "GeoSail: An Elegant Solar Sail Demonstration Mission," *Journal of Spacecraft and Rockets*, Vol. 44, No. 4, 2007, pp. 784–796. doi:10.2514/1.22867

[8] Wie, B., "Solar Sail Attitude Control and Dynamics: Parts 1 and 2," *Journal of Guidance, Control, and Dynamics*, Vol. 27, No. 4, 2004, pp. 526–544. doi:10.2514/1.11134

[9] Leipold, M., Garner, C. E., Freeland, R., Herrmann, A., Noca, M., Pagel, G., Seboldt, W., Sprague, G., and Unckenbold, W., "ODISSEE-A Proposal for Demonstration of a Solar Sail in Earth Orbit," *Acta Astronautica*, Vol. 45, Nos. 4–9, 1999, pp. 557–566. doi:10.1016/S0094-5765(99)00176-9

[10] Lyngvi, A., Rando, N., Marsden, R., Jeanes, A., Owens, A., Gerlach, L., Janin, G., and Peacock, A., "The Solar Orbiter," 56th IAC, International Astronautical Federation Paper IAC-05-C2.6.02, 2005.

[11] Macdonald, M., Hughes, G., McInnes, C., Lyngvi, A., Falkner, P., and Atzei, A., "Solar Polar Orbiter: A Solar Sail Technology Reference Study," *Journal of Spacecraft and Rockets*, Vol. 43, No. 5, Sept.–

Oct. 2006, pp. 960–972.
doi:10.2514/1.16408

[12] Goldstein, B. E., Buffington, A., Cummings, A. C., Fisher, R. R., Jackson, B. V., Liewer, P. C., Mewaldt, R. A., and Neugebauer, M., "Solar Polar Sail Mission: Report of a Study to Put a Scientific Spacecraft in a Circular Polar Orbit About the Sun," *Missions to the Sun II*, Proceedings of SPIE: The International Society for Optical Engineering, Vol. 3442, SPIE, Bellingham, WA, Nov. 1998, pp. 65–76.

[13] Montgomery, E., and Johnson, C., "The Development of Solar Sail Propulsion for NASA Science Missions," 45th AIAA/ASME/ASCE/AHS/ASC Structures, Structural Dynamics and Materials Conference, Palm Springs, CA, AIAA Paper 2004-1506, Apr. 2004.

[14] Dachwald, B., Ohndorf, A., and Wie, B., "Solar Sail Trajectory Optimization for the Solar Polar Imager (SPI) Mission," AIAA/AAS Astrodynamics Specialist Conference and Exhibit, Keystone, CO, AIAA Paper 2006-6177, Aug. 2006.

[15] Leipold, M., Lappas, V., Lyngvi, A., Falkner, P., Fichtner, H., and Kraft, S., "Interstellar Heliopause Probe: System Design of a Solar Sail Mission to 200 AU," AIAA Guidance, Navigation, and Control Conference, San Francisco, AIAA Paper 2005-6084, Aug. 2005.

[16] Lyngvi, A., Falkner, P., Kemble, S., Leipold, M., and Peacock, A., "The Interstellar Heliopause Probe," *Acta Astronautica*, Vol. 57, 2005, pp. 104–111.
doi:10.1016/j.actaastro.2005.03.042

[17] Fiehler, I. D., and McNutt, R. L., "Mission Design for the Innovative Interstellar Explorer Vision Mission," *Journal of Spacecraft and Rockets*, Vol. 43, No. 6, 2006, pp. 1239–1247.
doi:10.2514/1.20995

[18] Wie, B., "Solar Sailing Kinetic Energy Interceptor (KEI) Mission for Impacting and Deflecting Near-Earth Asteroids," AIAA Guidance, Navigation, and Control Conference and Exhibit, San Francisco, AIAA Paper 2005-6175, Aug. 2005.

[19] Lappas, V., Wie, B., McInnes, C., Tarabini, L., Gomes, L., and Wallace, K., "Microsolar Sails for Earth Magnetotail Monitoring," *Journal of Spacecraft and Rockets*, Vol. 44, No. 4, 2007, pp. 840–848.
doi:10.2514/1.23456

[20] Murphy, D. M., Murphey, T. W., and Gierow, P. A., "Scalable Solar-Sail Subsystem Design Concept," *Journal of Spacecraft and Rockets*, Vol. 40, No. 4, 2003, pp. 539–547.
doi:10.2514/2.3975

[21] Lichodziejewski, D., Derbes, B., Sleight, D., and Mann, T., "Vaccum Deployment and Testing of a 20-m Solar Sail System," 47th AIAA/ASME/ASCE/AHS/ASC Structures, Structural Dynamics, and Materials, Newport, RI, AIAA Paper 2006-1705, May 2006.

[22] Wie, B., and Murphy, D., "Solar-Sail Attitude Control Design for a Flight Validation Mission," *Journal of Spacecraft and Rockets*, Vol. 44, No. 4, 2007, pp. 809–821.
doi:10.2514/1.22996

[23] Lappas, V., Wie, B., McInnes, C., Tarabini, L., Gomes, L., and Wallace, K., "A Solar Kite Mission to Study the Earth's Magnetotail," *Journal of the British Interplanetary Society*, Vol. 58, Nos. 1–2, Jan.–Feb. 2005, pp. 23–31.

[24] Schwartz, S. J., "Solar Wind and the Earth's Bow Shock," *Solar System Magnetic Fields*, edited by E. R. Priest, D. Reidel, Boston, 1985, pp. 190–223.

[25] *Vega User's Manual*, Issue 2, Arianespace, Evry-Courcouronnes Cedex, France, Sept. 2004.

[26] Gil-Fernández, J., "Guidance Scheme for Autonomous Electric Propelled Spacecraft," International Astronautical Federation Paper IAC-93-A.208, Sept. 2003.

[27] Gil-Fernandez, J., "Optimization and Guidance of Very Low-Thrust Transfers to Geostationary Orbit," 57th IAC Congress, Valencia, Spain, International Astronautical Federation Paper IAC-06-C1.4.01, 2006.

[28] Gil-Fernandez, J., and Corral, C., "Exomars Alternative Escape Trajectories with Soyuz/Fregat," *Annals of the New York Academy of Sciences*, Advances in Astrodynamics and Applications, Vol. 1065, New York Academy of Sciences, New York, Dec. 2005.

[29] Camino, O., "Smart-1 Operations Experience and Lessons Learnt," 57th International Astronautical Congress, Valencia, Spain, International Astronautical Federation Paper 06-B5.3.08, Oct. 2006.

[30] Prieto-Llanos, T., "Genetic Algorithms in the Generation of an Initial Guess for the Optimization of Ascent Trajectories with a Hybrid Method," *5th International Conference on Launcher Technology*, Centre National d'Etudes Spatiales, Paris, Nov. 2003.

[31] Sovey, J., Carney, Lynnette, M., and Knowles, S., "Electromagnetic Emission Experiences Using Electric Propulsion Systems," *Journal of Propulsion and Power*, Vol. 5, No. 5, 1989, pp. 534–547.
doi:10.2514/3.23187

[32] Mengali, G., Quarta, A., and Lappas, V., "Optimal Steering Law for the GeoSail Mission," *Journal of Guidance, Control, and Dynamics*, Vol. 30, No. 3, May–June 2007, pp. 876–879.
doi:10.2514/1.28765

[33] Schmidt, T., Seifart, K., Burger, F., and Eder, J., "In Orbit Bonding (IOB) of Long Deployable Structures," *Proceedings of the 10th European Space Mechanisms and Tribology Symposium*, SP-524, ESA, Paris, 24–26 Sept. 2003, pp. 365–370.

[34] Laue, G., Case, D., and Moore, J., "Fabrication and Deployment Testing of Solar Sail Quadrants for a 20-Meter Solar Sail Ground Test System Demonstration," 41st AIAA Joint Propulsion Conference, AIAA Paper 2005-3930, July 2005.

[35] Johnson, L., Young, R., and Montgomery, E., "Recent Advances in Solar Sail Propulsion Systems at NASA," *Acta Astronautica*, Vol. 61, Nos. 1–6, June–Aug. 2007, pp. 76–382.

[36] Cawthorne, A., "The Next Generation DMC Small Satellite Platform for Earth Observation," 56th International Astronautical Congress of the International Astronautical Federation, Fukuoka, Japan, International Astronautical Federation Paper IAC-05-B5.4.01, Oct. 2005.

[37] Coxhill, I., and Gibbon, D., "A Xenon Resistojet Propulsion System for Microsatellites," 41st AIAA/ASME/SAE/ASEE Joint Propulsion Conference and Exhibit, Tucson, AZ, July 2005, AIAA Paper 2005-4260.

B. Marchand
Associate Editor